



## Research Article

# ***NUSAP1* and *PCLAF* (*KIA0101*) Downregulation by Neoadjuvant Therapy is Associated with Better Therapeutic Outcomes and Survival in Breast Cancer**

**Gerardo I. Magallanes-Garza,<sup>1,2,3</sup> Sandra K. Santuario-Facio,<sup>1</sup> Saúl Lira-Albarrán,<sup>4</sup> Arlina F. Varela-Varela,<sup>5</sup> Servando Cardona-Huerta,<sup>6,7</sup> Pablo Ruiz-Flores,<sup>5</sup> Jorge Haro-Santa-Cruz,<sup>5</sup> Yadira X. Perez-Paramo,<sup>8</sup> Gabriela Sofia Gomez-Macias,<sup>3,9</sup> Daniel Davila-Gonzalez,<sup>1,6</sup> Javier Valero-Gomez,<sup>1</sup> Gissela Borrego-Soto,<sup>10</sup> Augusto Rojas-Martinez <sup>1,4,11</sup> and Rocio Ortiz-Lopez <sup>1,4,11</sup>**

<sup>1</sup>Tecnologico de Monterrey, Escuela de Medicina y Ciencias de La Salud, Monterrey, Mexico

<sup>2</sup>Tecnologico de Monterrey, Servicio de Ginecología y Obstetricia, Tec Salud, Monterrey, Mexico

<sup>3</sup>Tecnologico de Monterrey, Centro de Cancer de Mama, Hospital Zambrano Hellion, San Pedro Garza Garcia, Mexico

<sup>4</sup>Tecnologico de Monterrey, The Institute for Obesity Research, Monterrey, Mexico

<sup>5</sup>Universidad Autonoma de Coahuila, Centro de Investigacion Biomedica, Facultad de Medicina, Unidad Torreon, Torreon, Mexico

<sup>6</sup>Tecnologico de Monterrey, Direccion Nacional de Investigacion Clinica TecSalud, Monterrey, Mexico

<sup>7</sup>Instituto Mexicano Del Seguro Social, Unidad Medica de Alta Especialidad No. 25, Monterrey, Mexico

<sup>8</sup>Washington State University, Pharmaceutical Sciences Department, College of Pharmacy Spokane, WA, USA

<sup>9</sup>Universidad Autonoma de Nuevo Leon, Facultad de Medicina, Monterrey, Mexico

<sup>10</sup>University of Texas at Austin, Department of Molecular Biosciences, Austin, TX, USA

<sup>11</sup>Universidad Autonoma de Nuevo Leon, CIDICS, Monterrey, Mexico

Correspondence should be addressed to Rocio Ortiz-Lopez; [rortizl@tec.mx](mailto:rortizl@tec.mx)

Received 8 June 2021; Revised 30 September 2022; Accepted 31 October 2022; Published 28 November 2022

Academic Editor: Tian Li

Copyright © 2022 Gerardo I. Magallanes-Garza et al. This is an open access article distributed under the Creative Commons Attribution License, which permits unrestricted use, distribution, and reproduction in any medium, provided the original work is properly cited.

**Purpose.** To evaluate whether changes in genomic expression that occur beginning with breast cancer (BC) diagnosis and through to tumor resection after neoadjuvant chemotherapy (NCT) reveal biomarkers that can help predict therapeutic response and survival. **Materials and Methods.** We determined gene expression profiles based on microarrays in tumor samples from 39 BC patients who showed pathologic complete response (pCR) or therapeutic failure (non-pCR) after NCT (cyclophosphamide-doxorubicin/epirubicin). Based on unsupervised clustering of gene expression, together with functional enrichment analyses of differentially expressed genes, we selected *NUSAP1*, *PCLAF*, *MME*, and *DST*. We evaluated the NCT response and the expression of these four genes in BC histologic subtypes. In addition, we study the presence of tumor-infiltrating lymphocytes. Finally, we analyze the correlation between *NUSAP1* and *PCLAF* against disease-free survival (DFS) and overall survival (OS). **Results.** A signature of 43 differentially expressed genes discriminated pCR from non-pCR patients ([fold change >2], false discovery rate <0.05) only in biopsies taken after surgery. Patients achieving pCR showed downregulation of *NUSAP1* and *PCLAF* in tumor tissues and increased DFS and OS, while overexpression of these genes correlated with poor therapeutic response and OS. These genes are involved in the regulation of mitotic division. **Conclusions.** The downregulation of *NUSAP1* and *PCLAF* after NCT is associated with the tumor response to chemotherapy and patient survival.

## 1. Introduction

Therapeutic response and prognosis in breast cancer (BC) are affected by such factors as patient age [1], clinical stage [2], tumor histopathology, and molecular subtypes [3]. Gene expression signatures performed before therapy can provide additional information on tumor biology, and algorithms have been developed to predict the risk of relapse and survival and define the best treatment options [4–6]. A program of genomic testing may allow for identifying low-risk tumors associated with a favorable prognosis. Also, it would facilitate therapeutic decision-making for aggressive tumors that respond poorly to conventional therapies. In this regard, transcriptional signatures can identify gene expression patterns related to chemotherapy resistance, immune system response, and tumor invasion [7–10].

Comparisons of gene expression analyses of biopsy specimens taken before and after neoadjuvant chemotherapy treatment (NCT) may help define tumor molecular adaptations to a specific chemotherapeutic agent or regime [7–10]. The pathologic complete response (pCR) in BC is defined as the absence of all invasive tumor tissue in the breast and axillary lymph nodes after the completion of NCT cycles [11, 12]. The achievement of pCR after NCT correlates with patient survival [12]. Alternative treatment regimens may improve survival when pCR is not achieved [13]. Comparisons of the changing patterns of transcriptional signatures in response to chemotherapy may enable predictions of clinical response and prognosis and, sometimes, recognize new response biomarkers of specific canonical pathways related to treatment resistance and recurrence.

No genomic signature defines therapeutic alternatives in patients with incomplete pathologic response (non-pCR). Therefore, the identification of gene expression profiles in tumor tissue after NCT that are associated with a good or an inadequate pathological response or with survival could facilitate the identification of patients who could benefit from second-line adjuvant treatment or improve clinical follow-up, as has been shown in some studies assessing pathologic response [14]. In addition, a review of the canonical pathways in which these genes are involved could also provide potential therapeutic targets or identify markers for high-risk patients who require closer follow-up.

This work aimed to analyze changes in genomic expression in primary BC tumors in patients undergoing NCT and to identify genes associated with prognosis in non-responding patients. These potential biomarkers could guide new pharmaceutical interventions for the second line of treatment. After validation, our studies showed that downregulation of *NUSAP1* and *PCLAF* (Previous Symbol HGNC: *KIAA0101*) and overexpression of *MME* and *DST* in tumor biopsies of patients significantly correlated with pCR after NCT disease-free survival (DFS) and overall survival (OS). *NUSAP1* is involved in cell proliferation and migration, and *PCLAF* participates in cell cycle control and apoptosis [15, 16]. Overexpression of these genes has each been correlated with tumor progression and metastasis [17, 18].

Downregulation of *MME* is associated with tumor recurrence and metastasis [19]. Underexpression of *DST*, which produces a cytoskeletal protein, promotes breast cancer progression independently of tumor hormonal status [20].

## 2. Materials and Methods

**2.1. Patient Population.** Patients with BC were enrolled in the study at the Centro de Cancer de Mama (Breast Cancer Center) Hospital San Jose TecSalud in Monterrey, Mexico. The Institutional Review Board of the School of Medicine of Tecnológico de Monterrey (CONBIOETICA 19 CEI 011-2016-10-17) authorized the research protocol with the number: P000088-Altru-Pro-CI-CR002. Following the Declaration of Helsinki, informed written consent was obtained from all patients participating in this study. Tissue samples were collected from 54 patients with clinical and/or radiologic diagnoses of BC (tumor size >2 cm and palpable lymph nodes) from July 2011 to October 2014.

**2.2. Neoadjuvant Chemotherapeutic Regimens.** Regimens were established according to the clinical stage and the immunohistochemistry of the breast tumors by medical oncologists. They consisted of 4 cycles every three weeks of either intravenous cyclophosphamide (500–1500 mg/m<sup>2</sup>) and doxorubicin (≥40 mg/m<sup>2</sup>) or intravenous cyclophosphamide (500–1500 mg/m<sup>2</sup>) and epirubicin (≥60 mg/m<sup>2</sup>). After receiving either of these regimens, patients received 12 weekly cycles of intravenous paclitaxel (80 mg/m<sup>2</sup>) administered over 1 hr [21]. In patients who demonstrated drug toxicity, cycles of carboplatin replaced the drug responsible for the toxicity [22]. Subsequently, surgical resection of the breast was performed on each patient. Some patients received selected adjuvant therapy after NCT (46% tamoxifen and 15% trastuzumab), as recommended by the attending oncologist. In such cases, the chemotherapeutic drug was chosen according to individual patient characteristics and clinical guidelines (e.g., trastuzumab and tamoxifen).

**2.3. Tumor Sample Collection.** Two tissue samples were collected from each patient: a biopsy sample (BS) before NCT and a surgery sample (SS) collected after completing the cycles of NCT. Thick needle puncture biopsies were obtained using a Bard Magnum 12 Fr gauge needle. Tumor location was marked at diagnosis using the carbon tracking technique [23]. Six to eight tissue cylinders were obtained from each patient. Four samples were used for histopathologic analysis, and three pieces were preserved in RNAlater solution (Sigma-Aldrich; Burlington, MA) for genomic analysis. The SS were obtained from surgeries for local-regional control (modified radical mastectomy in most cases). Tissues were sent to pathology for histopathologic and immunohistochemistry analysis. In addition, a 2 × 1 cm piece, marked by the carbon track used during the diagnostic biopsy procedure, was preserved in RNAlater solution for the gene expression analysis.

**2.4. Immunohistochemistry Analysis and Assessment of Tumor-Infiltrating Lymphocytes in BC Samples.** Samples were obtained from each patient for hematoxylin-eosin staining and immunohistochemistry for estrogen receptor (ER), progesterone receptor (PR), and HER2/neu. The histologic grade of the core needle biopsies was obtained before neoadjuvant therapy using the Bloom-Richardson scores [24]. The stage of breast cancer was determined according to the American Joint Committee on Cancer [25]. The percentage of tumor-infiltrating lymphocytes (TILs) was assessed following the International TILs Working Group 2014 in breast cancer [26]. A complete methodology for TIL assessment has been previously described [27]. Immunohistochemistry for CD3<sup>+</sup>, CD4<sup>+</sup>, and CD8<sup>+</sup> was also performed on the core needle biopsies before NCT to define lymphocyte immunophenotypes, following the American Society of Clinical Oncology/College of American Pathologists guidelines [28].

**2.5. Treatment Response.** One pathologist evaluated surgical specimens and assessed tumor response to NCT using the Miller–Payne grading system. For this study, a Miller–Payne grade 5 score was pCR, and the remaining scores (including partial pathologic response) were classified as non-pCR [29].

**2.6. RNA Isolation and Microarray Hybridization.** RNA isolation from BS and SS was prepared using RNeasy Fibrous Tissue Mini Kit (Qiagen; Germantown, MA) following the manufacturer's instructions. RNA quality was assessed by capillary electrophoresis using the Experion Automated Electrophoresis Station (Bio-Rad; Hercules, CA). Processing and microarray hybridization from the selected RNA samples were conducted using the GeneChip 3' IVT Express Kit (Thermo Fisher Scientific; Waltham, MA) and GeneChip Human Genome U133 Plus 2.0 Array (Applied Biosystems; Santa Clara, CA), according to manufacturer's instructions and as previously described [30, 31].

**2.7. Microarray Data Processing.** Normalization was performed using robust multiarray average (RMA) [32]. Probes with a mean expression <3 (logarithmic scale derived from RMA) were also removed from the further analysis. The differential gene expression analysis was performed using a *t*-test with multiple comparison corrections using the false discovery rate (FDR) method [33]. We considered the probes positive with an FDR <0.05. The differentially expressed genes (DEGs) were those with |fold change (FC) >2| and FDR <0.05 in every contrast evaluated. These analyses were completed using the free Applied Biosystems Transcriptome Analysis Console (TAC) 4.0.1 software (Thermo Fisher Scientific).

**2.8. Functional Enrichment Analysis.** The functional enrichment analysis was performed using g:Profiler  $\beta$  (version e106\_e53\_p16\_12c39de) with the g:SCS multiple testing correction methods, applying a significance threshold of 0.05 [34] and uploading the list of DEGs from every contrast

evaluated. The nomenclature of molecular functions, biological processes, and cellular components used the terms of the Gene Ontology Consortium [35]. In addition, the enriched canonical pathways were identified using KEGG [36], Reactome [37], and WikiPathways [38].

**2.9. Ingenuity Pathway Analysis.** The core analysis generated with QIAGEN IPA (QIAGEN Inc., <https://digitalinsights.qiagen.com/IPA>, accessed on 17 September 2022) identified the enriched bio-functions and canonical pathways (*p* – value < 0.01 using the right-tailed Fisher's exact test) defined by the Ingenuity Knowledge Base as well as the networks with the highest number of molecules involved [39] using the list of DEGs. Additionally, based on a hypothesis-driven approach to DEGs' effect on the regulation of mitosis, a molecule activity predictor analysis (MAP) by IPA was done.

**2.10. Real-Time qPCR Validation.** To validate microarray data, we selected four genes based on the microarray differential gene expression results and the functional enrichment analysis with g:Profiler  $\beta$  and IPA: two overexpressed genes (*MME* and *DST*) and two underexpressed genes (*NUSAPI* and *PCLAF*) in SS tissues. In addition, *GRAMD1A* was used as an endogenous gene control due to a low variation between samples [30]. Expression analyses were assessed using predesigned hydrolysis probes (*MME*, Hs00153510\_m1; *DST*, Hs00156137\_m1; *NUSAPI*, Hs01006195\_m1; *PCLAF*, Hs00207134\_m1; *GRAMD1A*, Hs.PT.5840681431) (Thermo Fisher Scientific and IDT for *GRAMD1A*). Total RNA aliquots used for microarray assays were analyzed through qPCR using the Applied Biosystems QuantStudio 3 Real-Time PCR System (Thermo Fisher). Cycle threshold (*Ct*) means for each gene were used to calculate  $\Delta Ct$  (problem minus endogenous), and  $2^{-\Delta Ct}$  analysis was done using calculated  $\Delta Ct$  for all genes. The gene expression of pCR and non-pCR groups was compared based on the relative expression  $2^{-\Delta Ct}$  evaluated from qPCR data from all genes after normalization with *GRAMD1A*. An unpaired *t*-test with Welch's correction was used to establish differences (*p* – value < 0.05).

**2.11. Evaluation of the Differences in Disease-free Survival and Overall Survival.** The SS gene expression values with DFS and OS were evaluated in 39 patients. In addition, the differences in OS were assessed based on a log-rank (Mantel-Cox) test that compares Kaplan–Meier survival curves [GraphPad Prism Windows version 6.01 (La Jolla, CA)]. A *p* – value < 0.05 was statistically significant.

For external validation, Kaplan–Meier Plotter (<https://kmplot.com/analysis/>) online database [40, 41] was used to analyze the OS correlated to high vs. low gene mRNA expression levels. The Kaplan–Meier Plotter split the BC patient (*n* = 1402) samples into two groups according to their median mRNA levels. The Affymetrix probe IDs used for the Kaplan–Meier analysis were *PCLAF* 202503\_s\_at and *NUSAPI* 219978\_s\_at.

TABLE 1: Clinical characteristics of patients included in the study.

	All patients ( <i>n</i> = 39)		pCR ( <i>n</i> = 8) (20.5%)		Non-pCR ( <i>n</i> = 31) (71.5%)		<i>p</i> - value
Age at diagnosis (years)	48	26 to 63	47	38 to 57	48	26 to 63	0.73
BMI (body mass index, kg/m <sup>2</sup> )	28.20	20.80 to 39.70	28.4	20.80 to 39.70	28.20	24.80 to 33.10	0.88
<25	8	20.51%	1	12.50%	7	22.58%	
>25	28	71.80%	6	75.00%	22	70.97%	
No data	3	7.69%	1	12.50%	2	6.45%	
Menopause status							
Pre	21	53.85%	5	62.50%	16	51.61%	0.88
Post	18	46.15%	3	37.50%	15	48.39%	
Family history							
Yes	19	48.72%	3	37.50%	16	51.61%	0.75
No	20	51.28%	5	62.50%	15	48.39%	
Diabetes mellitus							
Yes	2	5.13%	0	0.00%	2	6.45%	0.87
No	37	94.87%	8	100.00%	29	93.55%	
Number of children			3.6		3.2		0.44
Nulliparous	4	10.26%	0	0.00%	4	12.90%	0.22
1 or 2	12	30.77%	2	25.00%	10	32.26%	
>3	23	58.97%	6	75.00%	17	54.84%	
Lactation							
Yes	16	41.03%	3	37.50%	13	41.94%	0.97
No	11	28.20%	2	25.00%	9	29.03%	
No data	12	30.77%	3	37.50%	9	29.03%	
Smoking							
Yes	5	12.82%	2	25.0%	3	9.68%	0.25
No	34	87.18%	6	75.0%	28	90.32%	
Clinical stage							
I	1	2.56%	1	12.50%	0	0.00%	0.82
II	19	48.72%	2	25.00%	17	54.84%	
III	19	48.72%	5	62.50%	14	45.16%	
TNM classification							
T1	1	2.56%	1	12.50%	0	0.00%	0.93
T2	18	46.15%	1	12.50%	17	54.84%	
T3	11	28.21%	4	50.00%	7	22.58%	
T4	9	23.08%	2	25.00%	7	22.58%	
N0	7	17.95%	2	25.00%	5	16.13%	
N1	23	58.97%	4	50.00%	19	61.29%	
N2	9	23.08%	2	25.00%	7	22.58%	
M0	39	100.00%	8	100.0%	31	100.00%	
IHC markers							
ER+	16	41.03%	2	25.00%	14	45.16%	0.30
ER-	23	58.97%	6	75.00%	17	54.84%	
PR +	17	43.59%	2	25.00%	15	48.39%	0.23
PR-	22	56.41%	6	75.00%	16	51.61%	
HER2+	7	17.95%	5	62.50%	2	6.45%	0.002
HER2 -	32	82.05%	3	37.50%	29	93.55%	
ki67	15.40	5 to 70	17.14	5 to 50	14.92	2 to 70	0.76
Molecular subtype							
Luminal A	10	25.64%	1	12.50%	9	29.03%	0.51
Luminal B	6	15.39%	0	0.00%	6	19.36%	
HER2+	7	17.95%	5	62.50%	2	6.45%	
Triple-negative	16	41.02%	2	25.00%	14	45.16%	
<i>NUSAPI</i> (BS) <sup>a</sup>							
Overexpressed	17	43.59%	2	25.00%	15	48.39%	0.43
Underexpressed	22	56.41%	6	75.00%	16	51.61%	
<i>PCLAF</i> (BS) <sup>a</sup>							
Overexpressed	18	46.15%	4	50.00%	14	45.16%	>0.99

TABLE 1: Continued.

	All patients ( <i>n</i> = 39)		pCR ( <i>n</i> = 8) (20.5%)		Non-pCR ( <i>n</i> = 31) (71.5%)		<i>p</i> - value
Underexpressed	21	53.85%	4	50.00%	17	54.84%	
<i>NUSAP1</i> (SS) <sup>a</sup>							
Overexpressed	12	30.77%	0	0.00%	12	38.71%	0.04
Underexpressed	27	69.23%	8	100.00%	19	61.29%	
<i>PCLAF</i> (SS) <sup>a</sup>							
Overexpressed	28	71.80%	1	12.50%	29	93.55%	0.0001
Underexpressed	11	28.20%	7	87.50%	2	6.45%	

a *NUSAP1* or *PCLAF* were identified as overexpressed or underexpressed based on the contrast pCR vs. non-pCR in BS or SS samples as specified.

### 3. Results

**3.1. Patients.** Fifty-four patients were enrolled in the study, but only 44 paired (BS and SS) samples satisfied the RNA quality and quantity standards needed for the microarray analysis. In addition, five samples were eliminated because they failed to achieve quality standards after microarray hybridization, leaving 39 patient sample sizes for the final analyses. The clinical characteristics of the patients are described in Table 1. According to the Miller–Payne grading system, only 8 (20.5%) of the 39 patients reached pCR.

**3.2. Gene Expression Profile Analysis.** The following comparisons were made between SS and BS microarray data in pCR and non-pCR patients to assess the gene expression modifications induced by NCT: pCR-SS vs. pCR-BS (Supplementary Figure S1), non-pCR-SS vs. non-pCR-BS (Supplementary Figure S2), pCR-BS vs. and non-pCR-BS, and pCR-SS vs. non-pCR-SS (Figure 1).

**3.3. Functional Enrichment Analysis.** The first comparison pCR-SS vs. pCR-BS identified fourteen differentially expressed genes ( $|FC| > 2$ , FDR  $< 0.05$ , DEGs) (Supplementary File S1a). The overrepresentation analysis using this list of DEGs (Supplementary File S1b) included the molecular functions (MFs): DNA-binding transcription activator activity, RNA polymerase II-specific and the protein tyrosine/serine/threonine phosphatase activity. Interestingly, the identified enriched canonical pathway Nuclear Events (kinase and transcription factor activation) integrates the MFs overrepresented and highlight the effects of kinase and phosphatase activity on transcription factors. The second contrast non-pCR-SS vs. non-pCR-BS identified only four DEGs (Supplementary File S2a), and the unique MF overrepresented was nicotinamide phosphoribosyltransferase activity (Supplementary File S2b). No DEGs were identified in the third comparison pCR-BS vs. non-pCR-BS. The most interesting contrast was pCR-SS vs. non-pCR-SS, with a transcriptional signature of 43 DEGs (Supplementary File S3a). The overrepresented biological process: regulation of the mitotic cell cycle (Supplementary File S3b) suggests that this contrast could help us identify potential biomarkers associated with the clinical outcomes of breast cancer. So, we evaluated it by ingenuity pathway analysis (IPA).

**3.4. Ingenuity Pathway Analysis.** The core analysis by IPA using the list of 43 differentially expressed genes in the contrast pCR-SS vs. non-pCR-SS identified breast cancer as an enriched bio-function (Supplementary File S3c). In this regard, the most relevant enriched canonical pathways were cell Cycle: G2/M DNA damage checkpoint regulation, breast cancer regulation by Stathmin1, and molecular mechanisms of cancer (Supplementary File S3d). Interestingly, the MAP analysis based on the differential expression of some essential genes in the same contrast predicted inhibited bio-functions involved in breast cancer progression (Figure 2). For instance, the downregulation of *NUSAP1* and *PCLAF* inhibited mitosis and synthesis of DNA, respectively. The upregulation of *MME* inhibited the migration of cells, and the upregulation of *DST* activated the organization of the cytoskeleton. Furthermore, the MAP of mitosis bio-function predicted it as inhibited because of the downregulation of *NUSAP1* and *AURKA* that directly modified this critical process in cancer development. Indeed, *PCLAF* also influences mitosis by inhibiting *UBE2C* (Figure 3). In summary, the functional enrichment analysis identified *NUSAP1*, *PCLAF*, *MME*, and *DST* as potential biomarkers to be validated by RT-qPCR and evaluated in survival analyses.

**3.5. RT-qPCR Validation.** Four genes (*DST*, *MME*, *NUSAP1*, and *PCLAF*) were selected to validate the microarrays by RT-qPCR. Unfortunately, the remaining DNA from the tissue sample was scarce; therefore, only 31 (pCR = 5, non-pCR = 26) of 39 samples had enough quality and quantity of total RNA to perform this analysis. Supplementary Figure S3 shows the box plot of *NUSAP1* and *PCLAF* (Figures S3a and S3b, respectively) and *DST* and *MME* expression (Figures S3c and S3d, respectively). This analysis confirmed the expression patterns of these DEGs in the microarray.

**3.6. *NUSAP1* and *PCLAF* Gene Expression.** In the subset of patients achieving pCR, *NUSAP1* and *PCLAF* gene expressions were higher in the BS than in the SS samples (two-way ANOVA,  $F = 22.12$ ,  $p$  - value = 0.0053) (Figures 4(a) and 4(c)). In contrast, there was no significant difference in the expression values in the non-pCR groups (two-way ANOVA,  $F = 1.246$ ,  $p$  - value = 0.27) (Figures 4(b) and 4(d)). It is important to note that the

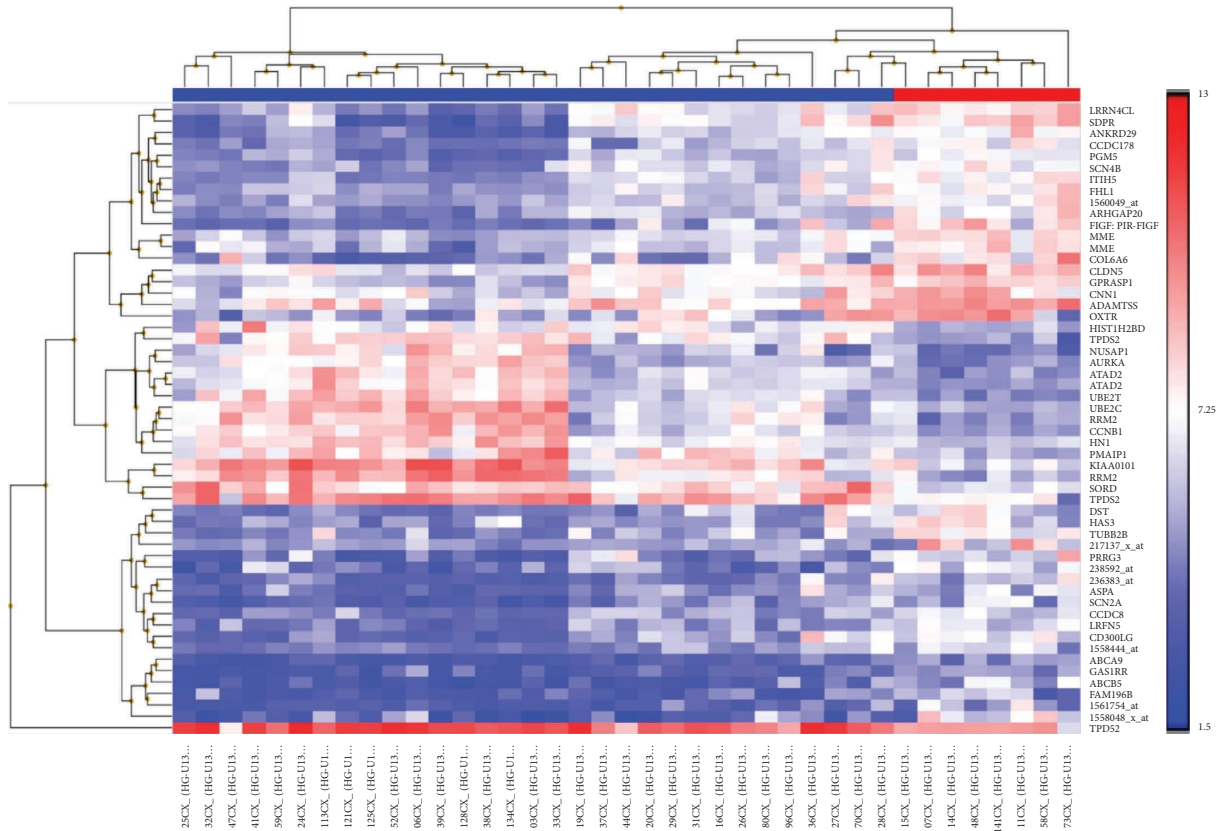


FIGURE 1: Unsupervised clustering of gene expression data in SS samples: pCR ( $n = 8$ ) vs. non-pCR ( $n = 31$ ). In the top row, pCR samples are denoted by the red header, and the blue title indicates non-pCR samples. The heatmap shows one sample for each column and one gene or probe for each horizontal line. The color indicates gene expression value intensities, where the gradient pink-red represents overexpression, and the gradient light blue-dark blue represents underexpression.

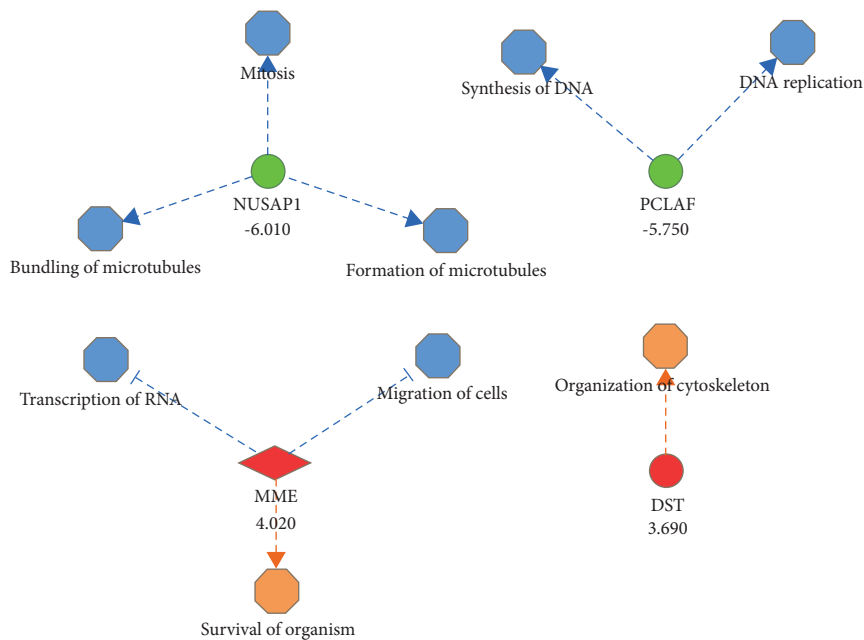


FIGURE 2: Molecule activity prediction of bio-functions associated with breast cancer using differentially expressed genes identified in the contrast pCR vs. non-pCR from SS samples. Colors indicated the predicted relationship between gene expression levels and bio-functions: green: down-regulated genes; red: up-regulated genes. Blue: bio-function inhibited; orange: bio-function activated. The blue line leads to inhibition; the orange line leads to activation. The fold change of every differentially expressed gene appears below from its gene symbol.

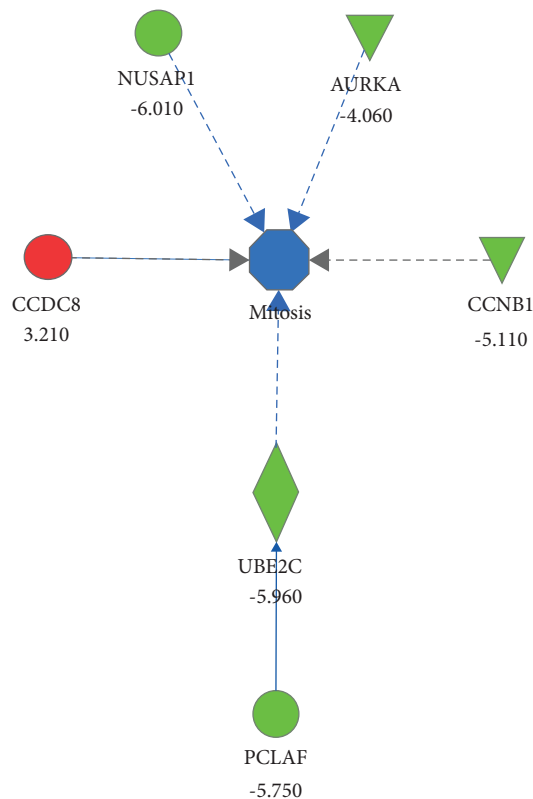


FIGURE 3: Molecule activity prediction of the mitosis biofunction using differentially expressed genes identified in the contrast pCR vs. non-pCR from SS samples. Colors indicated the predicted relationship between gene expression levels and biofunctions. Green: down-regulated genes; red: up-regulated genes. Blue: biofunction inhibited. The blue line leads to inhibition; the gray line indicates an effect not predicted. The fold change of every differentially expressed gene appears below from its gene symbol.

expression of *NUSAP1* after NCT was significantly higher in luminal B tumors than in the rest of the histologic subtypes (F test = 4.88,  $p$  - value = 0.006) (Supplementary Figure S4).

**3.7. Expression of *NUSAP1* and *PCLAF1* and Response to Treatment.** tResponse to NCT was considered the primary response variable and was evaluated using the Miller–Payne grading system. The association between the *NUSAP1* and *PCLAF* genes with response to treatment was tested. The expression of *NUSAP1* and *PCLAF* after NCT were inversely associated with pCR, implying that the downregulation of these genes had a favorable effect on the patient, as shown in Table 2 (*NUSAP1*: OR = 0.00, CI95% = 0.00–0.99,  $p$  = 0.0417; *PCLAF*: OR = 0.01, CI 95% = 0.0009–0.1383,  $p$  = 0.0001).

**3.8. Tumor-Infiltrating Lymphocytes (TILs) in BC Samples.** A correlation between TILs and gene expression levels of *NUSAP1* or *PCLAF* before NCT was not observed ( $r$  = 0.10,  $p$  = 0.65, 95% CI –0.39–0.25) or *PCLAF* ( $r$  = –0.07,  $p$  = 0.54, 95% CI –0.22–0.40). Representative images of TILs evaluation are shown in Supplementary Figure S5.

**3.9. Disease-free Survival and Overall Survival.** Patients were followed up for 46.5 months on average (SD = 20.34; range = 5.1–79.2 months). Supplementary Figure S6 shows that HER2+ patients have better overall survival, although significance levels were not reached ( $p$  - value = 0.07). *NUSAP1* and *PCLAF* expression patterns were compared against tumor relapse for disease-free survival and death due to BC for OS. Regarding DFS, the number of relapses was significantly higher in patients with overexpression of *NUSAP1* in the SS (38%, log-rank Mantel-Cox test,  $\chi^2$  = 4.67,  $p$  - value = 0.03) (Figure 5(a)). Likewise, higher levels of *NUSAP1* gene expression in the SS were also associated with decreased OS, with a reduction from 84% to 50% (log-rank Mantel-Cox test),  $\chi^2$  = 5.198,  $p$  - value = 0.02) (Figure 5(c)). Similarly, *PCLAF* overexpression negatively affected OS, with a reduction from 80% to 71% (log-rank Mantel-Cox test),  $\chi^2$  = 0.40,  $p$  - value = 0.53 (Figures 5(b) and 5(d)). Comparisons of gene expression patterns from BS failed to classify responders and no responders. OS results were replicated by analyzing public data on 1402 patients from the Kaplan–Meier Plotter website (<https://kmplot.com>) [40, 41]. Low levels of *NUSAP1* and *PCLAF* were associated with greater OS (log-rank HR = 1.82, CI95% = 1.46–2.26,  $p$  - value =  $6.2 \times 10^{-8}$  and log-rank HR = 1.47, CI95% = 1.19–1.82,  $p$ -value = 0.0004, respectively; Figures 5(e) and 5(f), respectively).

## 4. Discussion

Omics technologies, global gene expression analyses, in particular, have had a significant impact on the understanding of BC biology, the classification of pathologic subtypes, the design of predictive algorithms, and, most importantly, the discovery and implementation of new and more effective therapies to control this disease [42]. All these advances have positioned BC as one of the archetypal entities in precision medicine. Improvements in the selection of therapies based on the different molecular subtypes of BC have yielded higher DFS and prolonged OS. However, a high proportion of patients who do not fully respond to the assigned therapy has been observed after a particular treatment time. Therefore, choosing the appropriate therapeutic regimen at the beginning of treatment is crucial. Indeed, defining the most appropriate therapies beyond the first line is challenging, especially in pretreated patients [43]. Consequently, analysis of the molecular response to NCT may offer an opportunity to define prognoses and alternative therapies in patients with a BC diagnosis [12].

In this work, we studied gene expression profiles obtained through unsupervised cluster analysis of BS and SS tissues in patients with pCR and non-pCR after NCT. After evaluating the functional enrichment analysis of the different transcriptional signatures, the contrast pCR vs. non-pCR in SS tissues was the most attractive based on a hypothesis-driven approach to identify potential biomarkers associated with clinical outcomes. This analysis unveiled 30 overexpressed and 13 underexpressed genes in treated tumors (Supplementary File S3a). Seven of these genes enriched the regulation of the mitotic cell cycle (*AURKA*,



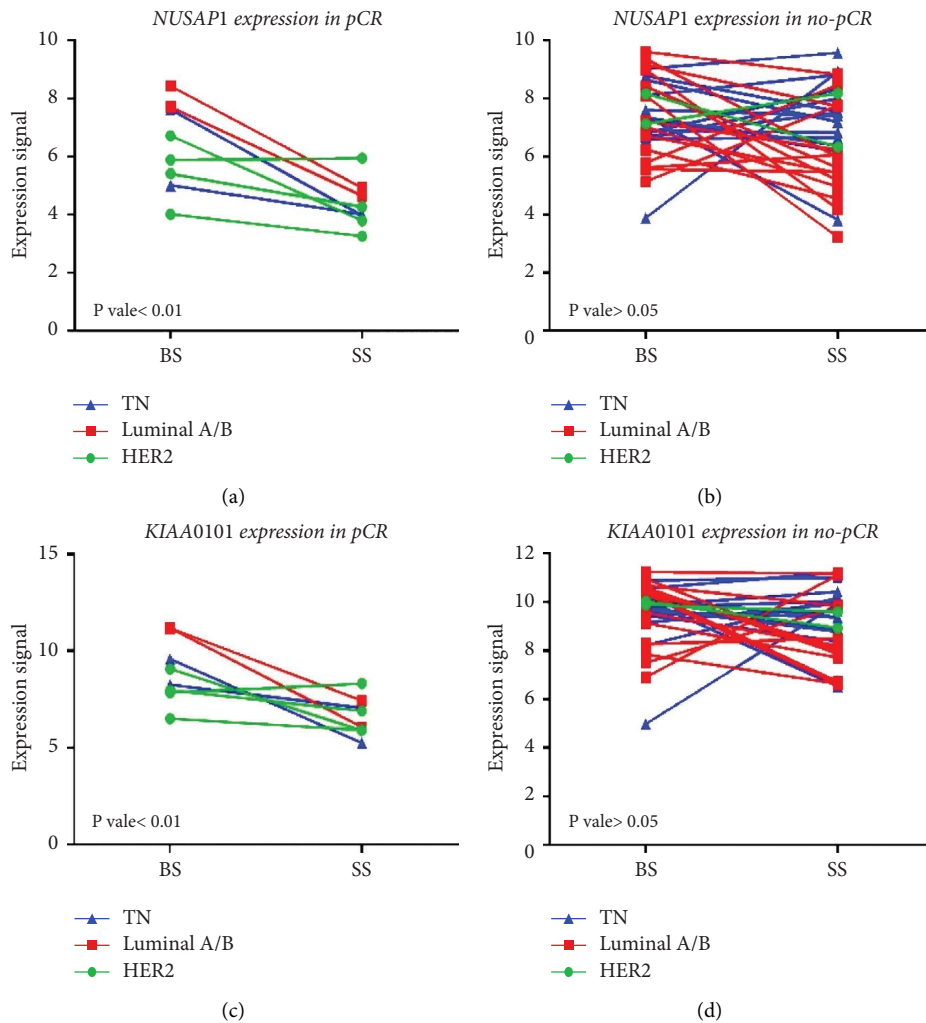


FIGURE 4: *NUSAP1* and *PCLAF/KIAA0101* gene expression based on microarray data. (a) *NUSAP1* gene expression in BS and SS in pCR and (b) non-pCR patients, respectively. (c) *PCLAF* (Previous symbol *KIAA0101*) gene expression in BS and SS in pCR and (d) non-pCR (d) patients, respectively. Blue lines and triangles, triple-negative molecular subtype; red lines and squares, luminal A/B molecular subtype; green lines and circles, HER2 molecular subtypes. Two-way ANOVA was performed, and a  $p$  - value < 0.05 was considered significant.

TABLE 2: *NUSAP1* and *PCLAF* and response to treatment.

	<i>NUSAP1</i>	<i>PCLAF</i>
OR	0.00	0.01
CI95%	0.000 to 0.991	0.0009 to 0.1383
$p$ -value	0.0417	0.0001
Sensitivity	0.00	0.13
CI95%	0.000 to 0.324	0.006412 to 0.4709
Specificity	0.61	0.06452
CI95%	0.438 to 0.763	0.01146 to 0.2072
Positive predictive value	0.00	0.03
CI95%	0.000 to 0.243	0.001710 to 0.1667
Negative predictive value	0.70	0.22
CI95%	0.515 to 0.842	0.03948 to 0.5474
Likelihood ratio	0.00	0.1336

*CCDC8*, *CCNB1*, *FHL1*, *NUSAP1*, *RRM2*, and *UBE2C*). Interestingly, *CCNB1*, *NUSAP1*, *RRM2*, and *UBE2C*, including *PCLAF* and *UBE2T*, are part of a transcriptional signature identified in BC from the Middle East young

women [44]. Moreover, *CCNB1*, *RRM2*, and *UBE2C* are included in the PAM50 signature for the molecular classification of BC lesions [45]. However, as far as we know, there are no reports of a genetic signature predicting BC response after NCT.

Some studies evaluating gene expression profiles and their association with a pCR have been already reported. For example, in Kolacinska's study in 2012, they analyzed biopsies from 42 patients before NCT (anthracyclines and taxanes) and identified seven differentially expressed genes (*BAX*, *CYP2D6*, *ERCC1*, *FOXC1*, *IRF1*, *MAP2*, and *MKI67*) in patients with pCR. We should note that this study performed target gene analysis rather than global expression analysis. The authors selected 23 genes according to their inclusion criteria and did not include prognostic value data or in-depth analysis of enriched signaling pathways in the comparisons [45].

On the other hand, an 80-Gene Molecular Subtyping Profile (Blueprint) was evaluated as a predictor of response



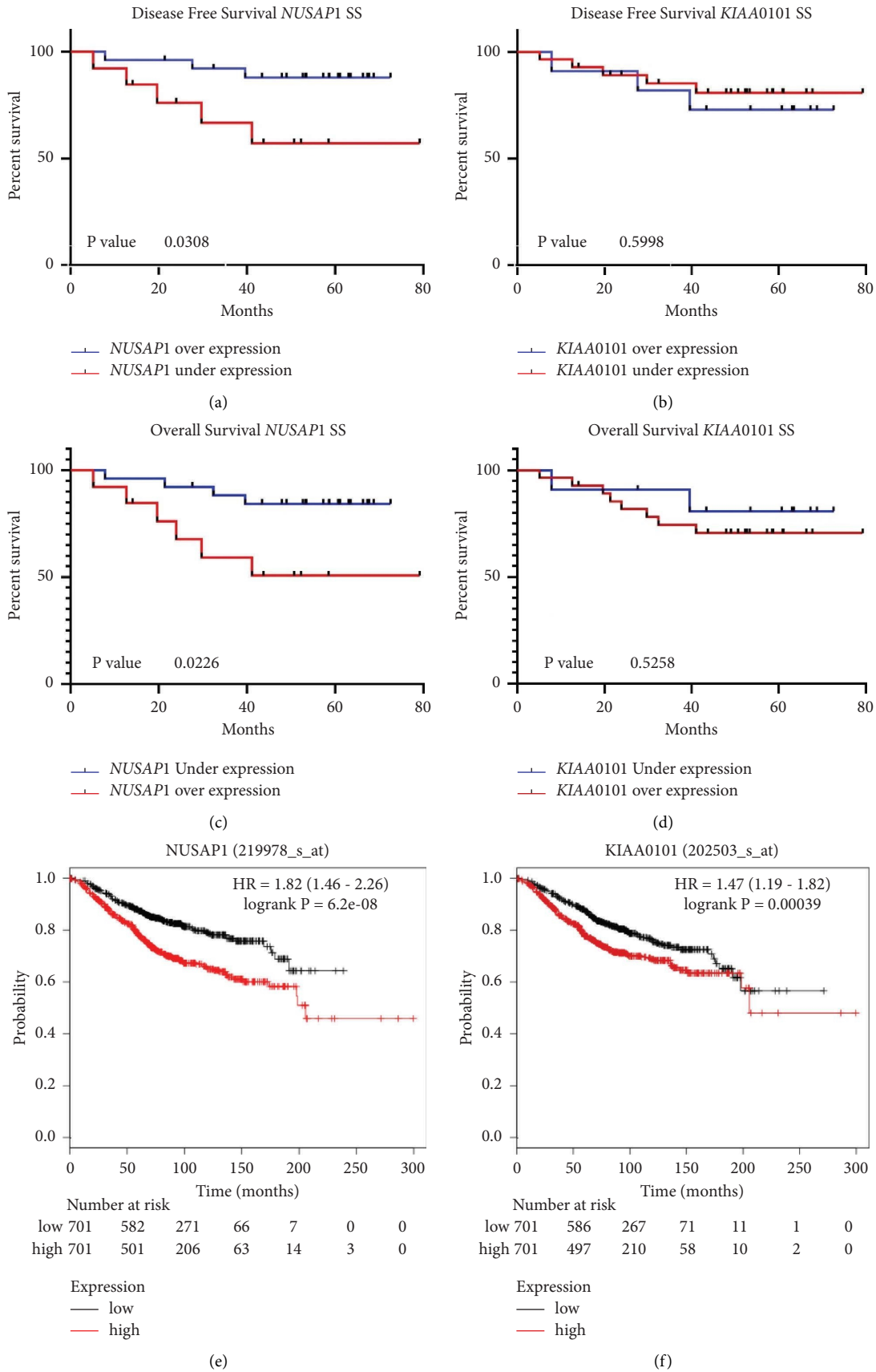


FIGURE 5: Disease-free survival and overall survival against *NUSAP1* and *PCLAF/KIAA0101* gene expression profiles in surgical samples (SS). (a-b) DFS curves considering *NUSAP1* and *PCLAF/KIAA0101* gene expression profiles after NCT (SS), respectively. Blue lines, underexpression; red lines, overexpression. (c-d) OS curves considering *NUSAP1* and *PCLAF/KIAA0101* gene expression profiles after NCT (SS), respectively. Blue lines, underexpression; red lines, overexpression. (e-f) OS curves considering *NUSAP1* and *PCLAF/KIAA0101* expression profiles from the Kaplan–Meier plotter website (<https://kmplot.com>), respectively. Black lines, underexpression; red lines, overexpression.

to chemotherapy in 133 patients treated with neoadjuvant chemotherapy (anthracyclines and taxanes). The results showed that the majority of patients with pCR were basal-type or Her2-enriched breast tumors. Of the 80 genes that make up BluePrint, 48 have coincidences with those described in the PAM50 gene set, in addition, Luminal-type tumors show gene enrichment in the estrogen receptor pathway [46]. In addition to these clinical approaches, computational reanalysis studies have been also carried out, such as the work reported by Zhao in 2020 where the response to NCT in patients, mostly with TNBC, is evaluated. In this work, response probability scores (RPS) were calculated to predict response to chemotherapy for TNBC and whose accuracy is higher than other previously reported signatures. These results are similar to those reported for ER-positive tumors using MammaPrint and Oncotype DX and reflect the activities of pathways, including cell cycle pathways, related to the immune system and ECM [46].

We selected four genes for RT-qPCR validation analyses based on the differential gene expression results in the microarray and the functional enrichment analysis using these DEGs identified in SS biopsies. Two chosen genes were overexpressed (*MME* and *DST*) and two more were underexpressed (*NUSAP1* and *PCLAF*). These validation studies corroborated the expression patterns observed in the microarray analyses. Interestingly, the gene expression levels of *NUSAP1* and *PCLAF* were more discriminating in the RT-qPCR analyses, so they were chosen to perform the DSF and OS studies (Supplementary Figure S3).

DSF and OS studies based on expression levels in SS demonstrated that low *NUSAP1* expression was associated with better DFS. Similarly, *NUSAP1* and *PCLAF* underexpression were associated with increased OS (Figures 5(a)–5(f)).

The most important observation of this study is that the pCR achieved with the NCT regimens (cyclophosphamide/doxorubicin or cyclophosphamide/epirubicin) is associated with a significant decrease in the gene expression levels of *NUSAP1* and *PCLAF*. The association between clinical outcomes and transcriptional profile is consistent with the fact that the expression of these genes is involved in mitosis and DNA replication, respectively (Figure 2), fundamental processes involved in cancer progression, as will be discussed later. As reported, this clinical response presupposes better DFS and OS [11]. Furthermore, higher expression levels of these same genes in the tumor biopsy before treatment (BS) were associated with poorer survival, indicating that these genes are potential predictors of survival in diagnostic biopsies.

Our study suggests that the HER2+ subtype responds favorably to NCT ( $p$  – value = 0.02) and that the luminal B subtype responds poorly, with no observed significant difference. Gene expression patterns of *NUSAP1* and *PCLAF* in different molecular subtypes of BC after NCT showed that *NUSAP1* was overexpressed in luminal B tumors compared to luminal A, HER2+, and triple-negative subtypes (Figure 4 and Supplementary Figure S4). Colak et al. reported overexpression of *NUSAP1* and *PCLAF* in ductal in situ and invasive ductal carcinoma compared to normal age-matched

controls [44]. Tumor-infiltrating lymphocytes have been reported to modulate the NCT response in breast cancer [47]. Furthermore, in the same study, no correlations were observed between TIL counts and gene expression (*NUSAP1* and *PCLAF*) in BS tissues from patients with and without PCR.

The protein PCNA-associated factor encoded by *PCLAF* binds the PCNA protein, acts as a regulator of the number of centrosomes, and is involved in DNA repair during DNA replication [15]. Overexpressed *PCLAF* has also been associated with decreased survival in BC patients [15] but not the pathologic response to NCT. Similarly, *NUSAP1* gene expression levels showed a remarkable inverse correlation with survival (Figures 5(a), 5(c), and 5(e)). This gene encodes for nucleolar and spindle-associated protein 1, which binds to chromatin and microtubules and is critical for the cytokinesis spindle assembly during mitosis [16]. *NUSAP1* overexpression has been reported in bladder, cervical, colon, liver, lung, prostate, kidney, and breast cancers, glioblastoma, and oral squamous cell carcinoma [48–52]; multiple studies have correlated its overexpression with poor prognosis [15, 49, 50, 53–57]. Zhang et al. demonstrated that the downregulation of *NUSAP1* suppressed proliferation, migration, and invasion of MCF-7 cells by disturbing the regulation of *CDK1* and *DLGAP5* and increasing susceptibility to epirubicin [50]. Our findings are like those of Qiu et al. They reported higher *NUSAP1* expression in tumors than in adjacent healthy tissue and an inverse correlation between *NUSAP1* expression and OS in BC patients. These findings were corroborated in a BALB/c-nu mouse model in which they determined the involvement of *NUSAP1* in tumor proliferation, migration, and invasion [18]. Finally, *NUSAP1* has been proposed as a carcinogenic element whose overexpression would help tumor progression in triple-negative BC cells, participating in the epithelial-mesenchymal transition and the Wnt/ $\beta$ -catenin pathways [17].

Our findings, together with those previously reported, indicate that these two genes may be prognostic genetic markers in BC but, at the same time, potential therapeutic targets. The proteins encoded by *NUSAP1* and *PCLAF* are involved in BCRA1-mediated DNA repair. *NUSAP1* increases *BRCA1* expression [58], whereas *PCLAF* regulates the number of centrosomes by interacting with *BRCA1* [15]. Since the biological roles of the *NUSAP1* and *PCLAF* involve cell cycle pathways, patients with elevated transcription levels of these genes may benefit from chemotherapeutic drugs interfering with *BRCA1*, such as platinum derivatives. *NUSAP1* overexpression could also be treated with galiellalactone, a fungal metabolite with antitumor and anti-inflammatory properties. Galiellalactone downregulates *NUSAP1* in DU 145 cells by targeting the NF- $\kappa$ B and STAT3 pathways, inducing cell cycle arrest [59]. Another option to target *NUSAP1* overexpression is the antitumor compound isopicrinine, isolated from *Rhazya stricta*, an inhibitor of the microtubule assembly [60].

Finally, decreased expression of *NUSAP1* seems to sensitize osteosarcoma cells to paclitaxel, as *NUSAP1* interacts with the RanBP2-RanGAP1-UBC9 SUMO E3 ligase

complex, allowing for accurate chromosomal segregation [61]. In addition, *NUSAPI* knockdown has been observed to potentiate paclitaxel-induced apoptosis in oral squamous cell carcinoma [62].

Our studies show significant results of the downregulation of *NUSAPI* and *PCLAF* and overexpression of *MME* and *DST* in SS, predicting pCR. BS data do not reach significance, but this correlation is also registered. On the contrary, the data suggest that overexpression of *NUSAPI* and *PCLAF* are associated with decreased DFS. This information could be useful to implement second-line treatment or more aggressive regimens in nonresponders.

It is essential to highlight some limitations of this study. The first is the small sample size; however, the NCT schemes and sampling were standardized for most study participants. The selection also has an overrepresentation of triple-negative BC because the NCT program prioritizes patients with this tumor subtype.

## 5. Conclusions

Downregulation of *NUSAPI* and *PCLAF* in SS after NCT was associated with favorable therapeutic response and prognosis in BC. These two genes represent potential biomarkers for personalized therapies for patients who do not respond adequately to NCT.

## Data Availability

The dataset generated and analyzed during the current study can be available from the corresponding author upon reasonable request.

## Ethical Approval

The Institutional Review Board from the School of Medicine of Tecnológico de Monterrey (CONBIOETICA 19 CEI 011-2016-10-17) authorized the research protocol with the number: P000088-Altru-Pro-CI-CR002. In accordance with the Declaration of Helsinki, informed written consent was obtained from all patients participating in this study.

## Disclosure

Gerardo I. Magallanes-Garza and Sandra K. Santuario-Facio are co-first authors.

## Conflicts of Interest

The authors declare that there are no conflicts of interest regarding the publication of this paper.

## Authors' Contributions

Gerardo I. Magallanes-Garza and Sandra K. Santuario-Facio conceptualized, developed methodology, investigated, wrote the original draft, and reviewed and edited the manuscript, and visualized the study; Saúl Lira-Albarrán analyzed functional enrichment and reviewed and edited the manuscript; Arlina F. Varela-Varela validated and investigated

the study; Servando Cardona-Huerta conceptualized the study, investigated the study, and reviewed and edited the manuscript; Pablo Ruiz-Flores Jorge, Haro-Santa-Cruz, Yadira X, Perez-Paramo, Javier Valero-Gomez, Gissela Borrego-Soto, and Gabriela S. Gomez-Macias validated and investigated the study; Daniel Davila-Gonzalez curated the data and visualized the study; Augusto Rojas-Martinez wrote the original draft, reviewed and edited the manuscript, and visualized the study; Rocio Ortiz-Lopez conceptualized the study, developed methodology, wrote the original draft, reviewed and edited the data, supervised the study, administered project, and acquired funding. Magallanes-Garza GI and Santuario-Facio SK are considered the first authors, as they both contributed equally to this manuscript.

## Acknowledgments

The authors thank Tecnológico de Monterrey, CONACYT, and the Center for Research and Development in Health Sciences (CIDICS) from the Autonomous University of Nuevo León (UANL). This work was supported by Tecnológico de Monterrey (Convocatoria para el Desarrollo de Protocolos de Investigación Clínica Sobre Temas Prioritarios para la Escuela de Medicina y Ciencias de la Salud 2018) and the Mexican National Council of Science and Technology (CONACYT) [SALUD 2011: 162301, 2017 APN: 4496].

## Supplementary Materials

*Supplementary Figure S1.* Heatmap of pCR samples: SS ( $n = 16$ ) vs. BS ( $n = 16$ ). In the top row, SS samples are denoted by the blue header, and the red title indicates BS samples. The heatmap shows one sample for each column and one gene or probe for each horizontal line. The color indicates gene expression value intensities, where the pink-red gradient represents overexpression, and the light blue–dark blue gradient represents underexpression. *Supplementary Figure S2.* Heatmap of non-pCR samples: SS ( $n = 31$ ) vs. BS ( $n = 31$ ). In the top row, BS samples are denoted by the blue header, and the red title indicates SS samples. The heatmap shows one sample for each column and one gene or probe for each horizontal line. The color indicates gene expression value intensities, where the pink-red gradient represents overexpression, and the light blue–dark blue gradient represents underexpression. *Supplementary Figure S3.* Box plots showing microarray selected genes validation by RT-qPCR (*NUSAPI*, *PCLAF1*, *DST*, and *MME*). a and b represent expression levels of *NUSAPI* and *PCLAF1*, respectively. c and d represent the expression of *DST* and *MME*, respectively. An unpaired *t*-test with Welch's correction was used for comparisons. *Supplementary Figure S4.* Expression levels of *NUSAPI* according to the molecular subtype after NCT (SS). LA, luminal A; LB, luminal B; TN = triple negative. One-way ANOVA and the Holm–Sidak multiple comparisons test were used for comparisons. *Supplementary Figure S5.* Microscopic evaluation of tumor-infiltrating lymphocytes (TILs). (a) Low TILs, 10 $\times$ . Fibrous stroma is observed between the tumor cells, with little lymphoplasmacytic infiltration at 5%. (b) Moderate TILs, 10 $\times$ .

Moderate lymphoplasmacytic infiltrate is seen in the tumoral stroma at 30%. (c) High TILs, 10×. A dense lymphoplasmacytic infiltrate was observed in the stroma between the neoplastic cells in the upper left area at 80%. *Supplementary Figure S6*. Overall survival according to the molecular subtype after NCT only in surgical samples. LA = luminal A, LB = luminal B, TN = triple negative. Log-rank (Mantel-Cox) test was used for comparisons. *Supplementary Figure S7*. Graphic abstract: Gene expression profiles based on microarrays were carried out in Breast Cancer (BC) tumor samples from Biopsy (BS) at the diagnostic time and from Surgery (SS) after neoadjuvant chemotherapy treatment (NCT) with cyclophosphamide-doxorubicin/epirubicin, to define tumor molecular adaptations to chemotherapy in patients who showed pathologic complete response (pCR) or therapeutic failure (non-pCR) after NCT. A signature of 43 differentially expressed genes discriminated pCR from non-pCR patients ( $|\log_2$  fold change  $>2$ ], false discovery rate  $<0.05$ ) only in biopsies taken from surgery. Based on unsupervised clustering of gene expression, together with functional enrichment analyses of differentially expressed genes, we selected *NUSAP1*, *PCLAF*. We also analyze the correlation between *NUSAP1* and *PCLAF* against disease-free survival (DFS) and overall survival (OS). Patients achieving pCR showed downregulation of *NUSAP1* and *PCLAF* in tumor tissues and increased DFS and OS, while overexpression of these genes correlated with poor therapeutic response and OS. These genes are involved in the regulation of mitotic division. Conclusions: the downregulation of *NUSAP1* and *PCLAF* after NCT is associated with the tumor response to chemotherapy and patient survival. *Supplementary File S1*. (a) List of fourteen differentially expressed genes (DEGs) in the comparison of pCR-SS vs. pCR-BS. (b) Functional enrichment analysis of this contrast using 14 DEGs. *Supplementary File S2*. (a) List of four differentially expressed genes in the contrast non-pCR-SS vs. non-pCR-BS. (b) Functional enrichment analysis of this comparison using 4 DEGs. *Supplementary File S3*. (a) List of forty-three differentially expressed genes in the comparison of pCR-SS vs. non-pCR-SS. (b) Functional enrichment analysis of this contrast using 43 DEGs. (c) Enriched bio-functions defined by the Ingenuity Knowledge Base. (d) Enriched canonical pathways defined by the Ingenuity Knowledge Base. (*Supplementary Materials*)

## References

- [1] C. Villarreal-Garza, J. E. Bargallo-Rocha, E. Soto-Perez-de-Celis et al., "Real-world outcomes in young women with breast cancer treated with neoadjuvant chemotherapy," *Breast Cancer Research and Treatment*, vol. 157, no. 2, pp. 385–394, 2016.
- [2] N. Reynoso-Noveron, C. Villarreal-Garza, E. Soto-Perez-de-Celis et al., "Clinical and epidemiological profile of breast cancer in Mexico: results of the seguro popular," *Journal of Global Oncology*, vol. 3, no. 6, pp. 757–764, 2017.
- [3] W. Haque, V. Verma, S. Hatch, V. Suzanne Klimberg, E. Brian Butler, and B. S. Teh, "Response rates and pathologic complete response by breast cancer molecular subtype following neoadjuvant chemotherapy," *Breast Cancer Research and Treatment*, vol. 170, no. 3, pp. 559–567, 2018.
- [4] M. J. van de Vijver, Y. D. He, L. J. van 't Veer et al., "A gene-expression signature as a predictor of survival in breast cancer," *New England Journal of Medicine*, vol. 347, no. 25, pp. 1999–2009, 2002.
- [5] S. Paik, S. Shak, G. Tang et al., "A multigene assay to predict recurrence of tamoxifen-treated, node-negative breast cancer," *New England Journal of Medicine*, vol. 351, no. 27, pp. 2817–2826, 2004.
- [6] C. Sotiriou, P. Wirapati, S. Loi et al., "Gene expression profiling in breast cancer: understanding the molecular basis of histologic grade to improve prognosis," *Journal of the National Cancer Institute*, vol. 98, no. 4, pp. 262–272, 2006.
- [7] L. Vera-Ramirez, P. Sanchez-Rovira, C. L. Ramirez-Tortosa, J. L. Quiles, M. Ramirez-Tortosa, and J. A. Lorente, "Transcriptional shift identifies a set of genes driving breast cancer chemoresistance," *PLoS One*, vol. 8, no. 1, Article ID e53983, 2013.
- [8] A. M. Gonzalez-Angulo, T. Iwamoto, S. Liu et al., "Gene expression, molecular class changes, and pathway analysis after neoadjuvant systemic therapy for breast cancer," *Clinical Cancer Research*, vol. 18, no. 4, pp. 1109–1119, 2012.
- [9] C. D. Savci-Heijink, H. Halfwerk, J. Koster, and M. J. Van de Vijver, "Association between gene expression profile of the primary tumor and chemotherapy response of metastatic breast cancer," *BMC Cancer*, vol. 17, no. 1, p. 755, 2017.
- [10] T. Foukakis, J. Lovrot, A. Matikas et al., "Immune gene expression and response to chemotherapy in advanced breast cancer," *British Journal of Cancer*, vol. 118, no. 4, pp. 480–488, 2018.
- [11] P. Sasanpour, S. Sandoughdaran, A. Mosavi-Jarrahi, and M. Malekzadeh, "Predictors of pathological complete response to neoadjuvant chemotherapy in Iranian breast cancer patients," *Asian Pacific Journal of Cancer Prevention*, vol. 19, no. 9, pp. 2423–2427, 2018.
- [12] G. von Minckwitz, M. Untch, J. U. Blohmer et al., "Definition and impact of pathologic complete response on prognosis after neoadjuvant chemotherapy in various intrinsic breast cancer subtypes," *Journal of Clinical Oncology*, vol. 30, no. 15, pp. 1796–1804, 2012.
- [13] N. Masuda, S. J. Lee, S. Ohtani et al., "Adjuvant capecitabine for breast cancer after preoperative chemotherapy," *New England Journal of Medicine*, vol. 376, no. 22, pp. 2147–2159, 2017.
- [14] M. Huang, J. O'Shaughnessy, J. Zhao et al., "Association of pathologic complete response with long-term survival outcomes in triple-negative breast cancer: a meta-analysis," *Cancer Research*, vol. 80, no. 24, pp. 5427–5434, 2020.
- [15] Z. Kais, S. H. Barsky, H. Mathsyaraja et al., "KIAA0101 interacts with BRCA1 and regulates centrosome number," *Molecular Cancer Research*, vol. 9, no. 8, pp. 1091–1099, 2011.
- [16] K. Ribbeck, A. C. Groen, R. Santarella et al., "NuSAP, a mitotic RanGTP target that stabilizes and cross-links microtubules," *Molecular Biology of the Cell*, vol. 17, no. 6, pp. 2646–2660, 2006.
- [17] L. Sun, C. Shi, S. Liu et al., "Overexpression of NuSAP1 is predictive of an unfavourable prognosis and promotes proliferation and invasion of triple-negative breast cancer cells via the Wnt/ $\beta$ -catenin/EMT signalling axis," *Gene*, vol. 747, Article ID 144657, 2020.
- [18] J. Qiu, L. Xu, X. Zeng et al., "NUSAP1 promotes the metastasis of breast cancer cells via the AMPK/PPAR $\gamma$  signaling pathway," *Annals of Translational Medicine*, vol. 9, no. 22, p. 1689, 2021.

- [19] M. Li, L. Wang, Y. Zhan et al., "Membrane metalloendopeptidase (MME) suppresses metastasis of esophageal squamous cell carcinoma (ESCC) by inhibiting FAK-RhoA signaling Axis," *American Journal Of Pathology*, vol. 189, no. 7, pp. 1462–1472, 2019.
- [20] P. B. Jain, P. S. Guerreiro, S. Canato, and F. Janody, "The spectraplaklin Dystonin antagonizes YAP activity and suppresses tumorigenesis," *Scientific Reports*, vol. 9, no. 1, Article ID 19843, 2019.
- [21] H. Gogas, D. Pectasides, I. Kostopoulos et al., "Paclitaxel and carboplatin as neoadjuvant chemotherapy in patients with locally advanced breast cancer: a phase II Trial of the Hellenic Cooperative Oncology Group," *Clinical Breast Cancer*, vol. 10, no. 3, pp. 230–237, 2010.
- [22] X. S. Chen, X. Nie, C. Chen et al., "Weekly paclitaxel plus carboplatin is an effective nonanthracycline-containing regimen as neoadjuvant chemotherapy for breast cancer," *Annals of Oncology*, vol. 21, no. 5, pp. 961–967, 2010.
- [23] G. Svane, "A stereotaxic technique for preoperative marking of non-palpable breast lesions," *Acta Radiologica: Diagnosis*, vol. 24, no. 2, pp. 145–151, 1983.
- [24] H. J. G. Bloom and W. W. Richardson, "Histological grading and prognosis in breast cancer; a study of 1409 cases of which 359 have been followed for 15 years," *British Journal of Cancer*, vol. 11, no. 3, pp. 359–377, 1957.
- [25] A. J. C. . o. Cancer, "The New Edition (7th) AJCC Staging System for Breast Cancer," *Staging Manual and the Future of TNM. Ann Surg Oncol*, vol. 17, pp. 1471–1474, 2010.
- [26] R. Salgado, C. Denkert, S. Demaria et al., "The evaluation of tumor-infiltrating lymphocytes (TILs) in breast cancer: recommendations by an International TILs Working Group 2014," *Annals of Oncology*, vol. 26, no. 2, pp. 259–271, 2015.
- [27] G. Gomez Macias, G. Molinar.Flores, C. Lopez Garcia et al., "Immunotyping of tumor-infiltrating lymphocytes in triple-negative breast cancer and genetic characterization," *Oncology Letters*, vol. 20, no. 5, p. 1, 2020.
- [28] M. E. Hammond, D. F. Hayes, and A. C. Wolff, "Clinical notice for American society of clinical oncology-college of American pathologists guideline recommendations on ER/PgR and HER2 testing in breast cancer," *Journal of Clinical Oncology*, vol. 29, no. 15, p. e458, 2011.
- [29] K. N. Ogston, I. D. Miller, S. Payne et al., "A new histological grading system to assess response of breast cancers to primary chemotherapy: prognostic significance and survival," *The Breast*, vol. 12, no. 5, pp. 320–327, 2003.
- [30] S. K. Santuario-Facio, S. Cardona-Huerta, Y. X. Perez-Paramo et al., "A new gene expression signature for triple negative breast cancer using frozen fresh tissue before neoadjuvant chemotherapy," *Molecular Medicine*, vol. 23, no. 1, pp. 101–111, 2017.
- [31] I. Gerardo, S. K. Magallanes-Garza, A. F. Varela-Varela, and S. Cardona-Huerta, "NUSAP1 and KIAA0101 Down-regulation by Neo-Adjuvant Therapy Is Associated with Better Outcome and Survival in Breast Cancer," , 2020.
- [32] R. A. Irizarry and B. Hobbs, "Exploration, normalization, and summaries of high density oligonucleotide array probe level data," *Biostatistics*, vol. 4, no. 2, pp. 249–264, 2003.
- [33] Y. Benjamini, D. Drai, G. Elmer, N. Kafkafi, and I. Golani, "Controlling the false discovery rate in behavior genetics research," *Behavioural Brain Research*, vol. 125, no. 1-2, pp. 279–284, 2001.
- [34] U. Raudvere, L. Kolberg, I. Kuzmin et al., "g:Profiler: a web server for functional enrichment analysis and conversions of gene lists (2019 update)," *Nucleic Acids Research*, vol. 47, no. W1, pp. W191–W198, 2019.
- [35] M. Ashburner, C. A. Ball, J. A. Blake et al., "Gene Ontology: tool for the unification of biology," *Nature Genetics*, vol. 25, no. 1, pp. 25–29, 2000.
- [36] M. Kanehisa and S. Goto, "KEGG: kyoto encyclopedia of genes and genomes," *Nucleic Acids Research*, vol. 28, no. 1, pp. 27–30, 2000.
- [37] M. Gillespie, B. Jassal, R. Stephan et al., "The reactome pathway knowledgebase 2022," *Nucleic Acids Research*, vol. 50, no. D1, pp. D687–D692, 2022.
- [38] M. Martens, A. Ammar, A. Riutta et al., "WikiPathways: connecting communities," *Nucleic Acids Research*, vol. 49, no. D1, pp. D613–D621, 2021.
- [39] A. Kramer, J. Green, J. Pollard, and S. Tugendreich, "Causal analysis approaches in ingenuity pathway analysis," *Bioinformatics*, vol. 30, no. 4, pp. 523–530, 2014.
- [40] B. Gyorffy, A. Lanczky, A. C. Eklund et al., "An online survival analysis tool to rapidly assess the effect of 22, 277 genes on breast cancer prognosis using microarray data of 1, 809 patients," *Breast Cancer Research and Treatment*, vol. 123, no. 3, pp. 725–731, 2010.
- [41] A. Lanczky and B. Gyorffy, "Web-based survival analysis tool tailored for medical research (KMplot): development and implementation," *Journal of Medical Internet Research*, vol. 23, no. 7, Article ID e27633, 2021.
- [42] M. Scimeca, N. Urbano, N. Toschi, E. Bonanno, and O. Schillaci, "Precision medicine in breast cancer: from biological imaging to artificial intelligence," *Seminars in Cancer Biology*, vol. 72, pp. 1–3, 2021.
- [43] V. Lorusso, A. Latorre, and F. Giotta, "Chemotherapy options beyond the first line in HER-negative metastatic breast cancer," *Journal of Oncology*, vol. 2020, Article ID 9645294, 17 pages, 2020.
- [44] D. Colak, A. Nofal, A. AlBakheet et al., "Age-specific gene expression signatures for breast tumors and cross-species conserved potential cancer progression markers in young women," *PLoS One*, vol. 8, no. 5, Article ID e63204, 2013.
- [45] R. R. Bastien, A. Rodriguez-Lescure, M. T. Ebbert et al., "PAM50 breast cancer subtyping by RT-qPCR and concordance with standard clinical molecular markers," *BMC Medical Genomics*, vol. 5, no. 1, p. 44, 2012.
- [46] Y. Zhao, E. Schaafsma, and C. Cheng, "Gene signature-based prediction of triple-negative breast cancer patient response to Neoadjuvant chemotherapy," *Cancer Medicine*, vol. 9, no. 17, pp. 6281–6295, 2020.
- [47] V. Sarradin, A. Lusque, T. Filleron, F. Dalenc, and C. Franchet, "Immune microenvironment changes induced by neoadjuvant chemotherapy in triple-negative breast cancers: the MIMOSA-1 study," *Breast Cancer Research*, vol. 23, no. 1, p. 61, 2021.
- [48] C. Kretschmer, A. Sterner-Kock, F. Siedentopf, W. Schoenegg, P. M. Schlag, and W. Kemmner, "Identification of early molecular markers for breast cancer," *Molecular Cancer*, vol. 10, no. 1, p. 15, 2011.
- [49] R. Liu, C. X. Guo, and H. H. Zhou, "Network-based approach to identify prognostic biomarkers for estrogen receptor-positive breast cancer treatment with tamoxifen," *Cancer Biology & Therapy*, vol. 16, no. 2, pp. 317–324, 2015.
- [50] X. Zhang, Y. Pan, H. Fu, and J. Zhang, "Nucleolar and spindle associated protein 1 (NUSAP1) inhibits cell proliferation and enhances susceptibility to epirubicin in invasive breast cancer cells by regulating cyclin D kinase (CDK1) and DLGAP5

- expression,” *Medical Science Monitor*, vol. 24, pp. 8553–8564, 2018.
- [51] Y. Zhe, L. Jiong, F. Guoxing et al., “Hepatitis B virus X protein enhances hepatocarcinogenesis by depressing the targeting of NUSAP1 mRNA by miR-18b,” *Cancer Biology & Medicine*, vol. 16, no. 2, pp. 276–287, 2019.
- [52] L. Chen, L. Yang, F. Qiao et al., “High levels of nucleolar spindle-associated protein and reduced levels of BRCA1 expression predict poor prognosis in triple-negative breast cancer,” *PLoS One*, vol. 10, no. 10, Article ID e0140572, 2015.
- [53] J. R. Head, P. C. MacDonald, and M. L. Casey, “Cellular localization of membrane metalloendopeptidase (enkephalinase) in human endometrium during the ovarian cycle,” *Journal of Clinical Endocrinology and Metabolism*, vol. 76, no. 3, pp. 769–776, 1993.
- [54] Z. Qian, Y. Li, J. Ma et al., “Prognostic value of NUSAP1 in progression and expansion of glioblastoma multiforme,” *Journal of Neuro-Oncology*, vol. 140, no. 2, pp. 199–208, 2018.
- [55] Z. Yu, X. M. Li, M. Huai, S. S. Cao, H. Y. Han, and H. T. Liu, “Expression of NUSAP1 and its relationship with prognosis in non-small cell lung cancer,” *Zhonghua Zhongliu Zazhi*, vol. 41, no. 7, pp. 522–526, 2019.
- [56] C. A. Gordon, X. Gong, D. Ganesh, and J. D. Brooks, “NUSAP1 promotes invasion and metastasis of prostate cancer,” *Oncotarget*, vol. 8, no. 18, pp. 29935–29950, 2017.
- [57] H. Yang, L. Zhou, J. Chen et al., “A four-gene signature for prognosis in breast cancer patients with hypermethylated IL15RA,” *Oncology Letters*, vol. 17, no. 5, pp. 4245–4254, 2019.
- [58] S. Kotian, T. Banerjee, A. Lockhart, K. Huang, U. V. Catalyurek, and J. D. Parvin, “NUSAP1 influences the DNA damage response by controlling BRCA1 protein levels,” *Cancer Biology & Therapy*, vol. 15, no. 5, pp. 533–543, 2014.
- [59] M. Garrido-Rodriguez, I. Ortea, M. A. Calzado, E. Munoz, and V. Garcia, “SWATH proteomic profiling of prostate cancer cells identifies NUSAP1 as a potential molecular target for Galiellalactone,” *Journal of Proteomics*, vol. 193, pp. 217–229, 2019.
- [60] Z. Gu and A. Zakarian, “Total synthesis of rhazinilam: axial to point chirality transfer in an enantiospecific Pd-catalyzed transannular cyclization,” *Organic Letters*, vol. 12, no. 19, pp. 4224–4227, 2010.
- [61] C. A. Mills, A. Suzuki, A. Arceci et al., “Nucleolar and spindle-associated protein 1 (NUSAP1) interacts with a SUMO E3 ligase complex during chromosome segregation,” *Journal of Biological Chemistry*, vol. 292, no. 42, pp. 17178–17189, 2017.
- [62] A. Okamoto, M. Higo, M. Shiiba et al., “Down-regulation of nucleolar and spindle-associated protein 1 (NUSAP1) expression suppresses tumor and cell proliferation and enhances anti-tumor effect of paclitaxel in oral squamous cell carcinoma,” *PLoS One*, vol. 10, no. 11, Article ID e0142252, 2015.